Desalination and Water Treatment
www.deswater.com

doi: 10.5004/dwt.2018.23078

129 (2018) 266–278
October

Degradation of toxic organic dyes in aqueous medium in greener ways: Exploring the utility of Indian Curry Leaf plant and the nanoparticles synthesized using it

Deepa Kumari[a,b], Tamanna Mallick[a], Pratap Padhy[b], Samiran Mondal[c,*], Abhijit Karmakar[a,*], Naznin Ara Begum[a,*]

[a]*Department of Chemistry, Visva-Bharati (Central University), Santiniketan 731 235, WB, India, Tel. +91 9002495569; email: abhijitkarmakar754@gmail.com (A. Karmakar), Tel. +91 9434431810; Fax: +91 3463261526; email: naznin.begum@visva-bharati.ac.in (N.A. Begum)*
[b]*Department of Environmental Studies, Visva-Bharati (Central University), Santiniketan 731 235, WB, India*
[c]*Department of Chemistry, Rammohan College, Kolkata-700 009, WB, India, Tel. +91 8240828779; email: samiranmondal1985@gmail.com*

Received 24 March 2018; Accepted 5 September 2018

ABSTRACT

Two protocols based on (1) the use of leaves of Indian Curry leaf plant (*Murraya koenigii* Spreng.) as the green adsorbent for toxic organic dye and (2) the use of monometallic Au and Ag nanoparticles (NPs) and bimetallic Ag/Au NPs (synthesized by the aqueous extract of leaves of Indian curry leaf plant) as the green catalysts for the toxic organic dyes such as Methylene blue, Nile blue and Methylene green have been developed. The protocols developed are very easy to operate and require very simple laboratory set-up. Moreover these protocols are applicable at room temperature and pressure thus minimizes the energy cost. In other words, our protocols represent a green chemical route toward the remediation of toxic organic dyes from aqueous medium.

Keywords: Organic dyes; Toxicity; Dye removal; Green adsorbent; Metal nanoparticles; Catalytic degradation

1. Introduction

Keeping the environment clean and safe has emerged as one of the main concerns for the modern society. At the same time, these are also the strategic priorities in the current research arena. Rapid industrialization brought the economic growth and social comforts but it also raised the concern for increasing environmental pollution and related health hazards. Environmental hazards such as water pollution or the contamination of the water bodies by the industrial wastes and other discharges are the threats to the living systems. There are several types of water toxicants or pollutants among which toxic organic dyes are note-worthy.

Organic dyes have extensive industrial applications. These dyes are used in the textile industries (most significantly) besides food products, cosmetics, pharmaceuticals and paper printing industries. These compounds are often toxic to the living systems and these toxicants are frequently found in industrial waste water. The highest amounts of varieties of such dyes are used by the textile industries.

There are several types of organic dyes depending upon their chemical structure, for example, azo, phthalocyanine, anthraquinone, quinone imine and xanthene dyes. However, the azo dyes are considered as the most effective and these type of dyes are easier to handle for industrial applications than dyes from natural sources but such naturally occurring

* Corresponding authors.

dyes are less hazardous and more costly. Among all other dyes used in various industries, the azo dyes are the major water contaminants [1]. Therefore, the waste water of the textile industries generally contains large amount of such aromatic nitrogenous compounds in addition to other toxic materials, for example, heavy metal ions. These types of water toxicants are considered as highly carcinogenic [1].

Removal of these toxicants from water is highly important and challenging job. Several research groups are working in this direction. The commonly used methods for the removal of dyes from industrial wastes can be classified into three types: (i) biological, (ii) chemical and (iii) physical methods.

Biological methods require large surface area and these methods are less manageable and controllable. Chemical methods, for example, electro-coagulation, flocculation, precipitation, complexation, ion exchange, electrochemical oxidation and photocatalytic degradation, etc. are often used for dye removal from waste water but these methods are not cost-effective and easy to operate. On the other hand, physical methods such as membrane filtration, nano-filtration, reverse osmosis and electro-dialysis are also not universally applicable and economic. In this context, adsorption process is often considered as the simple and effective physical method of choice for the removal of dyes from waste water [2,3] but adsorption process is not universally implementable. Thus, scientists are working to enhance the universal adaptability of the adsorption-based physical methods. Silica-based materials, such as MCM-41 [4], silica aerogels [5], MCM-41, MCM-48, MCM-58 [6] and nanoporous SBA-3 [7], are extensively used as the adsorbents for different types of dyes. Organic and inorganic moieties can be combined to produce organic–inorganic composites, which are efficiently used as the dye adsorbents. Recently, polyaniline nanotubes base/silica composite [8], PVC–zeolite composites [9] and flexible PVC-silica composites [10] were developed which adsorb Methylene blue dye on their surfaces effectively. However, such composite systems are not easy to synthesize and universally applicable, especially in case of large-scale application. Activated carbon is found to be an effective adsorbent for toxic organic compounds because of its high specific surface area and adsorption capacity but cost of activated carbon is high.

Hence, there is a continuous quest for the low-cost method of the production of activated carbon. Several waste products such as peel of fruits, leaves, saw dusts, coconut shells and other plant materials are explored in this direction [11,12]. Interestingly, such plant materials as whole are also used by several researchers for the adsorption of toxic metal ions and organic compounds [13]. These types of waste management adsorption processes are much cheaper and easier to apply but these processes need to be standardized for large-scale applications.

All these made us interested to explore a plant-based green adsorbent (GA) for the toxic organic dyes. There is a long history of the use of leaves of Indian curry leaf plant *(Murraya koenigii* Spreng. Family Rutaceae), in Indian cuisine. Moreover, these leaves are used in the Indian traditional medicine due to their wide spectrum of therapeutic activities [14]. Leaves of Indian curry leaf plant, commonly known as curry leaves, are very rich sources of exogenous antioxidants, for example, flavonoids and polyphenols besides tannic acid and gallic acid [15]. In the present work, our aim was to test the ability of the leaves of Indian curry leaf plant or curry leaves as the adsorbent for dyes and we have selected aqueous solution of Methylene blue (MB) as a model dye. During the course of the search, it was found that curry leaves were highly efficient in the adsorption of toxic dyes, such as Methylene blue (MB) (Fig. 1) from aqueous medium.

The colors of organic dyes are mainly due to the presence of N=N or C=N bonds in their chemical structures which are covalently linked with the chromophoric moieties. The presence of such chemical bonds increases the difficulty in their degradation [16,17]. Hence, scientists are continuously searching for new methods for the degradation of these toxic dyes. Nano-materials (e.g., metal nanoparticles) with their unique structure-dependent properties are emerging as a good promise in addressing this problem and offering solutions. Chemical degradation of these dyes to non-toxic compounds can be done in the presence of metal NPs as catalysts. Many reduction reactions of nitro-aromatics are reported to be catalyzed by Au and Ag NPs [18,19]. Recent studies also showed that Ag and Au NPs can effectively catalyze the reductive degradation of organic dyes to non-toxic compounds [20,21].

In this connection, metal NPs synthesized by green or biogenic routes using plant materials (as reducing and stabilizing agents) are very much note-worthy. Biocompatibility of such NPs is very high as no toxic chemicals are used for their synthesis. Various research groups have shown the effective use of green/biogenically synthesized metal NPs as the catalysts for the chemical degradation of toxic organic dyes [22–41]. Maham et al. [22] synthesized Ag/reduced graphene oxide/Fe_3O_4 nanocomposite using *Lotus Garcinii* leaf extract and showed the applicability of the synthesized nanocomposite as the recyclable nanocatalyst for the reduction of 4-nitrophenol and organic dyes [22]. Other types of nanocomposites such as Ag/Fe_3O_4 [23], Ag/reduced graphene oxide (RGO) [24], Ag, RGO/TiO_2 [25], Ag/zeolite [26], Ag/TiO_2 [27] synthesized using various plant materials showed excellent catalytic activity toward the degradation of varieties of organic dyes in water medium.

Vaccinium macrocarpon fruit extract was used by Khodadadi et al. [28] for the synthesis of Ag NPs supported on the surface of clinoptilolite which showed excellent catalytic activity for the reduction of organic dyes. Ag NPs synthesized by *Achillea millefolium* L. extract as reducing and stabilizing

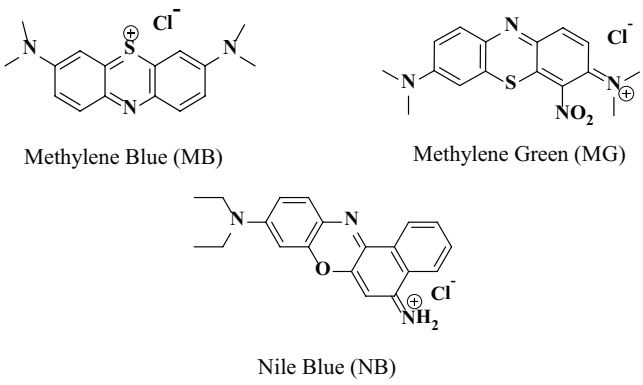

Fig. 1. Common organic dyes used for the present work.

agents and supported by peach kernel shell showed catalytic efficacy toward the degradation of various organic dyes [29]. Photocatalytic degradation of azo dyes was done by Rostami-Vartooni et al. [33] using titanium dioxide supported Ag NPs synthesized by *Carpobrotus acinaciformis* extract.

Biosynthesis of Ag, ZnO and Ag/ZnO alloy NPs was done by aqueous extract of oak fruit which showed photocatalytic activity toward the degradation of basic violet 3 dye [35]. Various research groups have successfully utilized wide spectrum of metal NPs by selecting plant-mediated biogenic synthetic routes and the synthesized NPs are successfully exploited as the effective catalysts for the chemical degradation of organic dyes [36–41].

These made us interested to synthesize metal NPs which can be used as the catalysts for the reductive degradation of organic dyes in aqueous medium.

Previously, the antioxidant activity of aqueous-methanolic extract of curry leaves in the synthesis of gold (Au) NPs [14] was explored. For the present work, monometallic Au and Ag NPs and bimetallic Ag/Au alloy NPs with finely tuned morphologies using aqueous extract of dried and pulverized leaves of Indian curry leaf plant as green multifunctional agent (GMA) (curry leaf extract acted both as reducing and stabilizing agents for the synthesized NPs) were synthesized and the catalytic activity of the synthesized NPs toward the reduction of Methylene blue (MB), Nile blue (NB) and Methylene green (MG) (Fig. 1) was studied.

2. Materials and methods

2.1. General experimental

2.1.1. Materials

Silver nitrate ($AgNO_3$) and chloroauric acid ($HAuCl_4$) (Sigma-Aldrich, Missouri, US) were used as a source of Ag^+ and $Au^{3+}$and ions required for the synthesis of monometallic Ag, Au and bimetallic Ag/Au NPs. All other chemicals used for the study were of analytical grade and Milli-Q (Milli-Q Academic with 0.22 mm Millipack R40) water was used as per requirements. Methylene blue (MB), Nile blue (NB) and Methylene green (MG) were purchased from Merck, India, and used without further purification.

2.1.2. Instrumentation

UV-visible spectroscopy was used to examine the formation and growth of the NPs as well as for the dye adsorption and catalytic degradation studies. Absorption spectra were recorded on Lambda 35 spectrophotometer (PerkinElmer, Massachusetts, US). The shape and size of the NPs were elucidated with the help of transmission electron microscopy (TEM). Samples for TEM were prepared by drop-coating method using carbon-coated copper grids (400 mesh size). The films on the grids were allowed to dry prior to the TEM measurement by a JEM-2100 instrument, JEOL, Tokyo, Japan.

2.2. Collection of leaves of Indian curry leaf plant and processing of curry leaves

Curry leaves were collected from our campus area (Visva-Bharati University, Santiniketan, West Bengal, India) during the month of July 2016. Leaves were washed with double distilled water for several times to make it free from dust and any dirt particles. Then the leaves were dried under shade. After that, the leaves were pulverized using mechanical grinder. The pulverized leaves were stored in air-tight container at 4°C for further use.

2.3. Batch adsorption experiments using leaves of Indian curry leaf plant or curry leaves as green adsorbent for toxic organic dyes

The pulverized leaves (i.e., curry leaf powder or CLP) were used as the green adsorbent for the organic dyes Methylene blue (MB), methylene green (MG) and Nile blue (NB). The batch adsorption technique was used to study the effects of various important parameters, such as amount of adsorbent, pH of the medium and the contact time between adsorbate (organic dyes) and adsorbent (CLP). To find out the optimum amount of adsorbent to be needed and pH value for the adsorption study, we selected Methylene blue (MB) dye as model adsorbate. The time parameter was studied to make a comparative adsorption study of MB, MG and NB.

To find out the optimum/effective dosage of the adsorbent, the following experiment was done: five sets of dye samples each containing 5 mL of aqueous solutions of MB (model adsorbate) having concentration of 0.5 g L^{-1} were taken. Then, CLP having concentrations of 2, 4, 6, 8 and 10 g L^{-1} was mixed individually with each of these dye samples. Then, each dye sample was stirred on magnetic stirrer for 90 min at 25°C. After that time period, each solution was filtered with Whatman 42 filter paper. The UV–Vis absorption spectra of the filtrates were recorded in the UV–Vis spectrophotometer to quantify the amount of un-adsorbed dye for these five sets of samples. Along with this, for the comparison purpose, a parallel blank study was also done using MB in the absence of CLP. For this experiment, the pH of the solutions was maintained at ~7, that is, neutral pH.

To study the effect of pH on the adsorption process, same experiment was repeated at different pH (4–9) values keeping the concentrations of MB and CLP fixed at 0.5 and 8 g L^{-1}, respectively. The pH of the solutions was adjusted by using either 1 M HCl or 1 M NaOH solutions.

For the comparative adsorption study, aqueous solution of each of the dyes, MB, MG and NB, having concentration of 0.5 g L^{-1} was diluted in 25 mL of water and to each of the dye sample, CLP (8 g L^{-1}) was added and subjected to stirring for 15 min. 3 mL of the aliquot from each sample was withdrawn at different time interval of times (15, 30, 60, 90, 120 and 150 min) and subjected to filtration. The absorbance of the filtrate for each of the dye samples was measured using UV–Vis spectrophotometer. The final concentrations of dyes were estimated with the help of these absorbance data (l_{max} for MB, MG and NB were 663, 658 and 634 nm, respectively).

The dye removal efficiency of GA was calculated as follows:

$$\text{Dye removal efficiency} = (C_i - C_t)/C_i \times 100 \quad (1)$$

where C_i is the initial concentration of dye and C_t is the concentration of dye at any particular time.

The amount of adsorption at equilibrium time, q_e (mg g^{-1}) was calculated using the following equation:

$$q_e = [(C_0 - C_e) \times V]/W \quad (2)$$

where C_0 is the liquid-phase concentrations of dye initially (mg L^{-1}); C_e is the liquid-phase concentrations of dye at equilibrium (mg L^{-1}); V represents the volume of the solution (L) and W is the mass of dry adsorbent used (g).

2.3.1. Determination of adsorption kinetics and adsorption isotherms

Adsorption isotherms are highly useful for determining the maximum adsorption capacity of any adsorbent. In the present case, to evaluate the adsorption capacity of the GA, that is, CLP, the Langmuir and Freundlich isotherm equations were explored.

2.3.1.1. Langmuir isotherm Langmuir adsorption isotherm is a very popularly used adsorption isotherm [42]. The linear form of this equation is shown below [43,44]:

$$1/q_e = 1/q_m K_a C_e + 1/q_m \quad (3)$$

where C_e is the concentration of adsorbate at equilibrium (mg L^{-1}); q_e is the amount of dye adsorbed at equilibrium (mg g^{-1}); q_m is the maximum adsorption capacity; K_a is the Langmuir constant.

2.3.1.2. Freundlich isotherm The Freundlich isotherm model describes the sorption of solute from liquid to solid surface and this model is based on the assumption that the stronger binding sites are occupied first and that the binding strength decreases with an increasing degree of site occupation [42]. This isotherm is described by the following equation [45]:

$$q_e = K_f C_e^{1/n} \quad (4)$$

where q_e is the amount of dye adsorbed per unit mass (mg g^{-1}); C_e is the equilibrium concentration (mg L^{-1}); n is the Freundlich linearity constant related to adsorption intensity and K_f is the Freundlich affinity coefficient related to adsorption capacity.

In our study, we have used the linear form of the above equation which is shown below:

$$\ln q_e = \ln K_f + 1/n \ln C_e \quad (5)$$

2.4. Method of extraction of curry leaves and synthesis of monometallic Ag, Au and bimetallic Au/Ag alloy NPs using aqueous extract of curry leaves

100 g of pulverized leaves were macerated in 1,200 mL of water in a closed container for 24 h at room temperature with occasional shaking. The extract was then filtered with Whatman No. 42 filter paper to remove any undissolved plant particles. After this, the extract was refluxed for 30 min. After this time period, the curry leaves aqueous extract (CAE) was again filtered and the solvent (water) was removed from the filtrate under reduced pressure using a rotary evaporator. After the complete removal of the solvent, a non-homogeneous, gummy mass (16 g) was obtained. The gummy mass was stored at 4°C and used further as GMA for the synthesis of NPs.

For the synthesis of Ag, Au and bimetallic Au/Ag alloy NPs, our previously reported method [14, 46,47] was followed. Here, a brief description was given.

The synthesis of Ag NP was done by adding of 100 μL of 0.05 M aqueous solution of $AgNO_3$ to 10 mL of aqueous solution of CAE (400 μg mL^{-1}) so that the final Ag^+ ion concentration in the reaction mixture became 0.5×10^{-3} M. A golden yellow coloration was developed within a minute which indicated the onset of Ag NP formation. The progress of the reaction was monitored by measuring the absorbance of reaction mixture at regular intervals of time using a UV–Vis spectrophotometer. The absorption peak was assigned as the surface plasmon resonance (SPR) band of Ag NP.

For Au NP synthesis, a similar method has been followed. In this case, we have added 100 μL of 0.05 M aqueous $HAuCl_4$ solution. In this case, the final concentration of Au^{3+} ions became 0.5×10^{-3} M. Within 5 min, a pink coloration was observed indicating the onset of Au NP formation.

Similarly, for bimetallic Ag/Au nanoparticles synthesis, 50 μL of 0.05 M aqueous $AgNO_3$ and 50 μL of 0.05 M aqueous $HAuCl_4$ solutions were added to 10 mL of aqueous solution of CAE (400 μg mL^{-1}) keeping other parameters unaltered. Characteristic color generation was observed within 5 min, which indicated the bimetallic alloy NP formation.

2.5. Reductive degradation of organic dyes by sodium borohydride using monometallic Ag, Au and bimetallic Au/Ag alloy NPs as catalysts

To test the catalytic efficacy of the synthesized NPs, the hydride transfer reduction reactions of dyes by $NaBH_4$ (sodium borohydride) were chosen. For this catalytic reduction, 60 μL of 5×10^{-4} M of a specific dye was added to 3.6 mL of water containing 75 μL of 0.9 M freshly prepared ice-cold $NaBH_4$. To this reaction mixture, 20 μL of Au NP solution was added and stirred by a magnetic stirrer at room temperature. Progress of the reaction was monitored by UV–Vis spectrophotometer. The catalytic ability of the Ag NP and bimetallic Ag/Au NP was also studied similarly. The degradation kinetics for all of the three dyes was studied with the Ag NPs only.

3. Results and discussion

3.1. Efficacy of the curry leaves as the green adsorbent for toxic organic dyes

3.1.1. Understanding the optimum amount for the green adsorbent

In general, the process of adsorption depends on the number of vacant sites at the surface of the adsorbent and by increasing the mass of the adsorbent, several sites become more available for the dye which is still dissolved in the solution. Fig. 2 illustrates that with the increment of adsorbent dosage, adsorption capacity was found to be increased. The removal percentage of MB was raised from 92.5% to 97.7% while the concentrations of adsorbent were increased from 2

to 8 g L^{-1}. It was interesting to note that the lower dosage of GA still showed appreciable adsorption capacity for these dyes. This may be due the high surface area and number of binding sites of the GA available for the dyes [48]. With the increase of concentration, the surface area and number of binding sites of the GA increased. Therefore, more amount of MB was adsorbed on the GA surface but this was found to be feasible up to a maximum concentration of 8 g L^{-1} of the GA. Beyond this concentration, no such effect was observed (Fig. 2).

3.1.2. Effects of pH on the adsorption capacity of curry leaves as green adsorbent

pH of the reaction mixture significantly affected the adsorption of dyes onto the surface of curry leaves based adsorbent. Dye removal percentage of MB was raised from 69.39% to 86.87% when the pH of the solution increased from acidic to neutral, that is, from ~4 to 7. At average pH, the more effective dye adsorption capacity of GA was observed. The optimum adsorption capacity was achieved at pH 7.2, that is, at the neutral condition. At lower pH, oxygen and nitrogen containing functional groups of the chemical constituents of curry leaves are protonated and thus the chelation power of GA decreased and also active sites of GA become less available for binding of the dye. As a result, removal efficiency of GA was found to be decreased (Fig. 3).

3.1.3. Effects of dye–green adsorbent contact time

Effects of the contact time on the adsorption process were studied and the results for all the dyes, MB, MG, NB, are shown in Figs. 4(a) (i and ii)–(c) (i and ii). From the results, it is clear that the removal efficiency of GA was found to be increased with increase of the contact time between the adsorbate, that is, dyes and the adsorbent, that is, GA. Fig. 4(a) (ii) shows that, initial removal of MB dye occurred very rapidly (~95% was removed within 60 min). After that, the rate became slow. It is due to the fact that the affinity of curry leaves or GA toward MB is so high that initially some of the easily available active sites got engaged and the dye needed some time to find out more vacant active sites for binding which made the whole process slow (Fig. 4(a) (ii)).

On the other hand, at first 30 min, a rapid removal was observed for both MG and NB with percentage of removal of 79.35% and 97.93%, respectively (Figs. 4(b) (ii) and (c) (ii)). Interestingly, the saturation level of MG and NB was reached after 150 min and 60 min, respectively (Figs. 4(b) (ii) and (c) (ii)).

The amount of dye adsorbed at equilibrium time, that is, q_e (mg g^{-1}) for all the dyes was calculated and the values are shown in Table 1. Here the contact time 180 min was taken as the equilibrium time for all the dyes at this particular time, the removal efficacy of the GA for all the dyes reached their saturation level. Highest value of q_e was obtained for NB suggesting the strong binding affinity between the organic functional groups of the chemical constituents of the curry leaves, that is, GA and the NB dye. MG and MB showed the similar q_e values due to the similarity in their structural patterns.

3.1.4. Adsorption isotherms

Adsorption isotherms are a major issue and play an important role in the determination of the maximum adsorption capacity of any adsorbent or the effective amount of the adsorbent during adsorption process. Adsorption isotherms also help to assess the possibility of the commercial and economic applications of an adsorbent for the removal of some specific solutes. For these reasons, we took the help of Langmuir and Freundlich isotherms to assess the adsorption capacity of our green adsorbent, curry leaves. Parameters of each isotherm were calculated using linear regression and the results are presented in Fig. 5.

3.2. Efficacy of the aqueous extract of the curry leaves or CAE toward the formation of monometallic Ag, Au and bimetallic Au/Ag alloy NPs

3.2.1. Formation and growth of monometallic Ag, Au and bimetallic Au/Ag alloy NPs

Appearance of characteristic color and SPR band in the UV-visible spectra of the NP solutions confirmed the formation of these NPs. Fig. S1(a) shows the result of the reaction between Ag^+ ions and the aqueous solution of CAE. Within 5 min of continuous stirring, the color of the reaction mixture

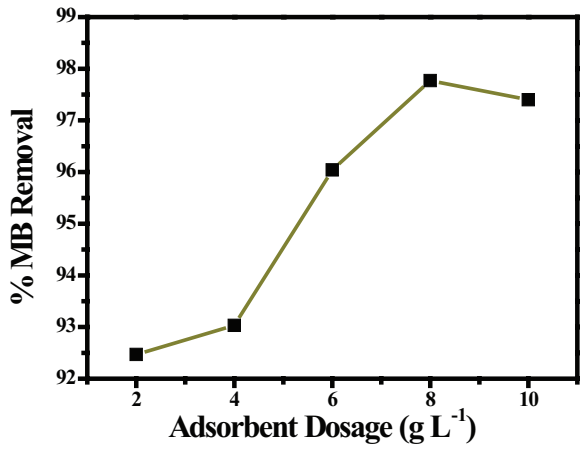

Fig. 2. Adsorption of Methylene blue (MB) dye using curry leaves as green adsorbent.

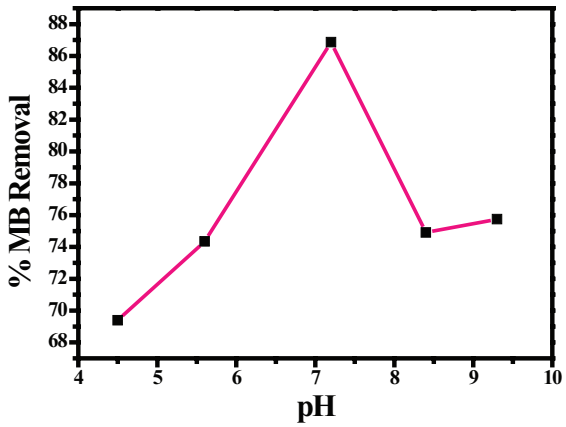

Fig. 3. Adsorption of Methylene blue (MB) dye onto curry leaves based green adsorbent at different pH (4.5, 5.6, 7.2, 8.4, 9.3) values.

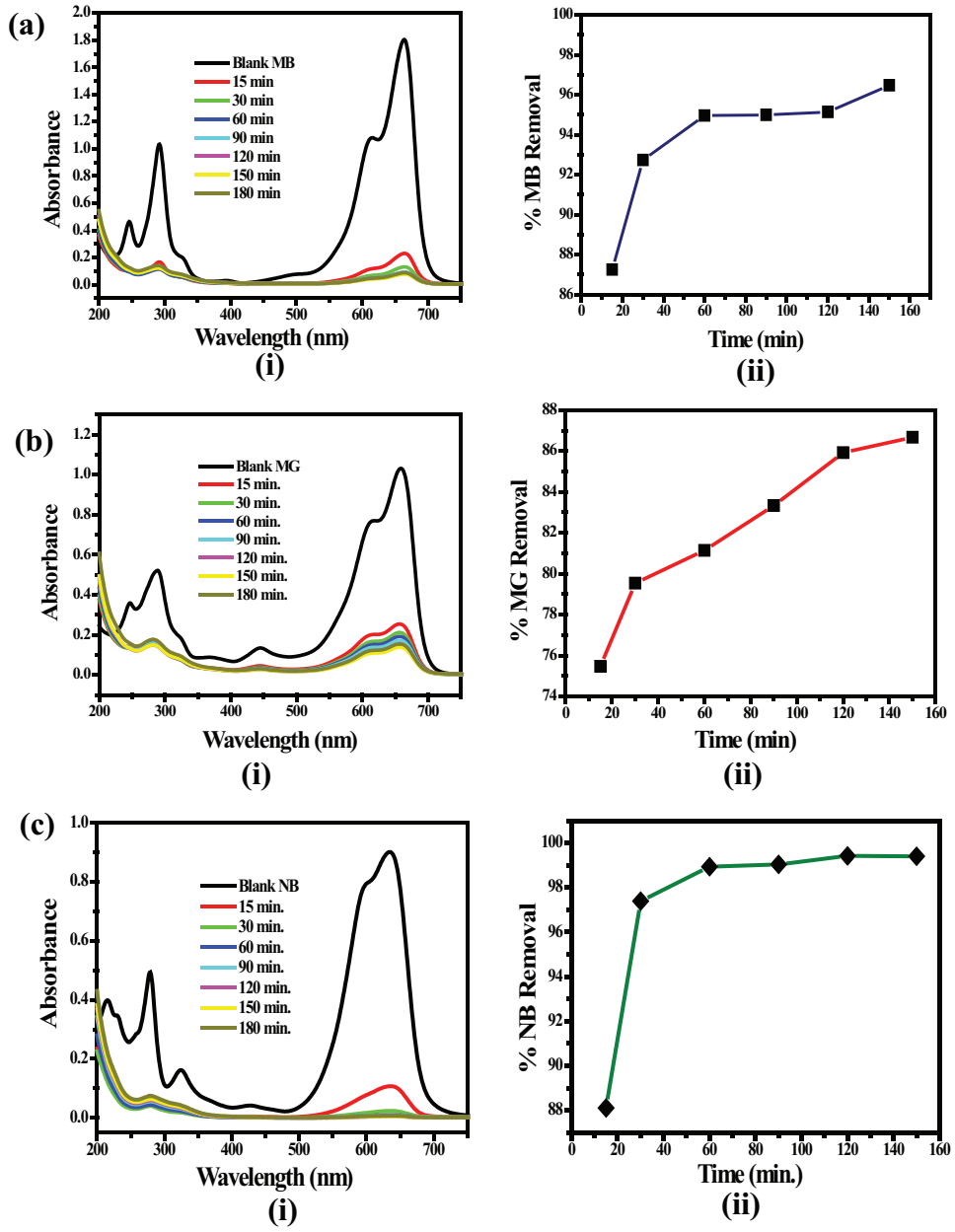

Fig. 4. Effect of contact time on the efficiency of curry leaves as green adsorbent in the adsorption of (a) MB, (b) MG, (c) NB dyes at pH ~ 7. Initial concentration of dyes was 0.5 g L^{-1} and amount of curry leaves used as green adsorbent was 8 g L^{-1}.

Table 1
Comparison of equilibrium time (q_e) values of the organic dyes adsorbed on GA surface

Organic dyes	q_e (mg g^{-1}) at equilibrium time
MB	59.46
MG	53.13
NB	118.96

turned to yellowish brown (inset of Fig. S1(a)) and SPR band for Ag NPs appeared at 457 nm.

Fig. S1(b) shows the formation of the Au NPs by reduction of Au^{3+} ions in presence of CAE and the reaction mixture turned pink-red (inset of Fig. S1(b)) within 5 min of addition of Au^{3+} ion. The appearance of a main peak at 541 nm with an additional peak at 761 nm was observed in this case. The dotted curves in each of Figs. S1(a) and (b) denote the absorption spectrum of the aqueous solution of CAE at $t = 0$, that is, in the absence of Ag^{+} or Au^{3+} ions. The appearance of the two absorption bands at longer and shorter wavelengths is due to the longitudinal and transverse surface plasmon oscillations [49]. This phenomenon is actually related to the anisotropy of the metal NPs formed [50].

CAE also showed its efficacy in the synthesis of Ag/Au bimetallic NPs by the simultaneous reduction of the Ag^{+} and Au^{3+} ions present in the same solution. In case of bimetallic Ag/Au alloy NPs formation, we observed only one

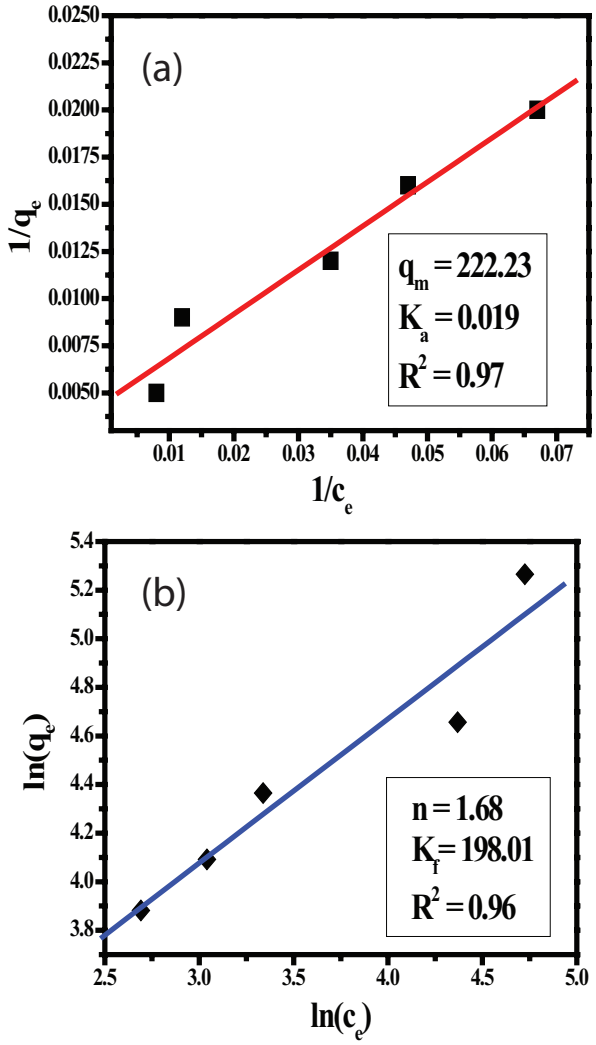

Fig. 5. (a) Langmuir adsorption isotherm and (b) Freundlich adsorption isotherm models for the adsorption of the dye, Methylene blue (MB) on the surface of curry leaves–based green adsorbent.

plasmon band in place of two individual bands for Ag and Au NPs [46].

Figs. S2(a)–(c) show absorption spectra of the bimetallic Ag/Au NPs. Detailed concentration range is given in Table 2.

In case of the monometallic Ag NP, the SPR band appeared at 457 nm whereas, for monometallic Au NP formation, dual SPR band was observed corresponding to the absorbance maxima at 541 nm (more intense) and 721 nm (less intense), respectively. In general, it is observed that, only one absorbance peak is obtained for each of the bimetallic nanoparticle solution [46]. Moreover, in all the cases, the absorbance maxima are found to be located at the positions in-between of those for monometallic Ag and Au NP SPR bands. This is in agreement with the previous reported data [51]. Simple physical mixture of monometallic Ag and Au NP solution does not give such absorption spectra. In Fig. S2, it is seen that for bimetallic Au/Ag NPs, the SPR band was obtained at 516 nm. This peak appeared almost at the middle position of two SPR bands of Ag and Au monometallic NPs.

Table 2
Synthesis of monometallic Ag, Au and bimetallic Ag/Au alloy NPs

System of NP	Concentration of Ag^+ (M)	Concentration of Au^{3+} (M)	Position of SPR band
Monometallic Ag	0.5×10^{-3}	0	457 nm
Bimetallic Ag/Au alloy	0.25×10^{-3}	0.25×10^{-3}	516 nm
Monometallic Au	0	0.25×10^{-3}	541 and 761 nm

3.2.2. Morphology of monometallic (Ag and Au) and bimetallic (Ag/Au) NPs synthesized by curry leaves aqueous extract

TEM images of the Ag NPs formed by CAE are mostly spheroidal in shape (Figs. S3(a) and (b)). On the other hand, Au NPs synthesized and stabilized by CAE have anisotropic structures besides regular spherical morphologies as shown in Figs. S3(c) and (d). Figs. S3(e) and (f) show the TEM images of the bimetallic Au/Ag NPs formed by the simultaneous reduction of Ag^+ and Au^{3+} ions in the (1:1) mixture by the CAE. In the close up view, it was observed that though particles are mostly spherical, occasional aggregations of the spherical particles existed. In the TEM images of the bimetallic Au/Ag nanoparticles, a uniform contrast for each NP was visible suggesting the existence of homogeneous electron density throughout the whole volume of the particle. So the bimetallic nanoparticles are not core/shell type and they bear a close resemblance to bimetallic alloy nanoparticles [50]. These results are in strong agreement with the UV-visible spectroscopic data discussed previously.

3.3. Efficacy of monometallic Ag, Au and bimetallic Au/Ag alloy NPs as catalysts toward the reductive degradation of organic dyes by sodium borohydride

In order to evaluate the catalytic activity of synthesized monometallic Ag, Au and bimetallic Ag/Au alloy NPs, the reduction of various dyes, MB, MG and NB by excess of $NaBH_4$ was investigated. Reduction of these dyes is indicated by the quenching of their absorption intensity (at λ_{max}) as these dyes showed characteristics peaks at different wavelengths in aqueous solution. These metal NPs with high surface area to volume ratio accelerated the reduction rate of the dyes. The degradation of MB, MG and NB by $NaBH_4$ into their corresponding reduced form in the presence of these metal NPs is depicted in Figs. 6((i)–(iii)).

Au NPs facilitated the transfer of electrons from the reducing agent ($NaBH_4$) to the substrates (dyes), thereby reduction of the dye solutions in presence of $NaBH_4$ occurred at a very faster rate. This higher catalytic activity may be due to the inert character of Au. Absorption profile of the catalytic activity of the Au NPs employed on the reduction of MB, MG and NB is shown in Fig. 6(i) ((a)–(c)).

In aqueous medium, MB, MG and NB show their characteristic absorption maxima at 664, 660 and 635 nm, respectively, as shown in Fig. 6(i) ((a)–(c)). The red colored curves of Fig. 6(i) ((a)–(c)) show the absorption spectra of

the reduction of MB, MG and NB by $NaBH_4$ in the absence of Au NPs which were recorded after 10 min of the addition of $NaBH_4$ and no change in absorbance of the dye solutions was observed. This indicated that these dyes were not reduced effectively by $NaBH_4$ or the reduction rate is very much slow in the absence of NP catalysts. Degradation of the dyes became very much faster when Au NPs were used as the catalysts and this was shown by the blue colored curves.

Compared with the catalytic activity of the synthesized Au NPs, Ag NPs showed slow reduction rate for the same $NaBH_4$ reduction of MB, MG and NB dye solutions. Ag NP takes longer time for the completion of the reduction of the various dyes owing to its lower catalytic potential than

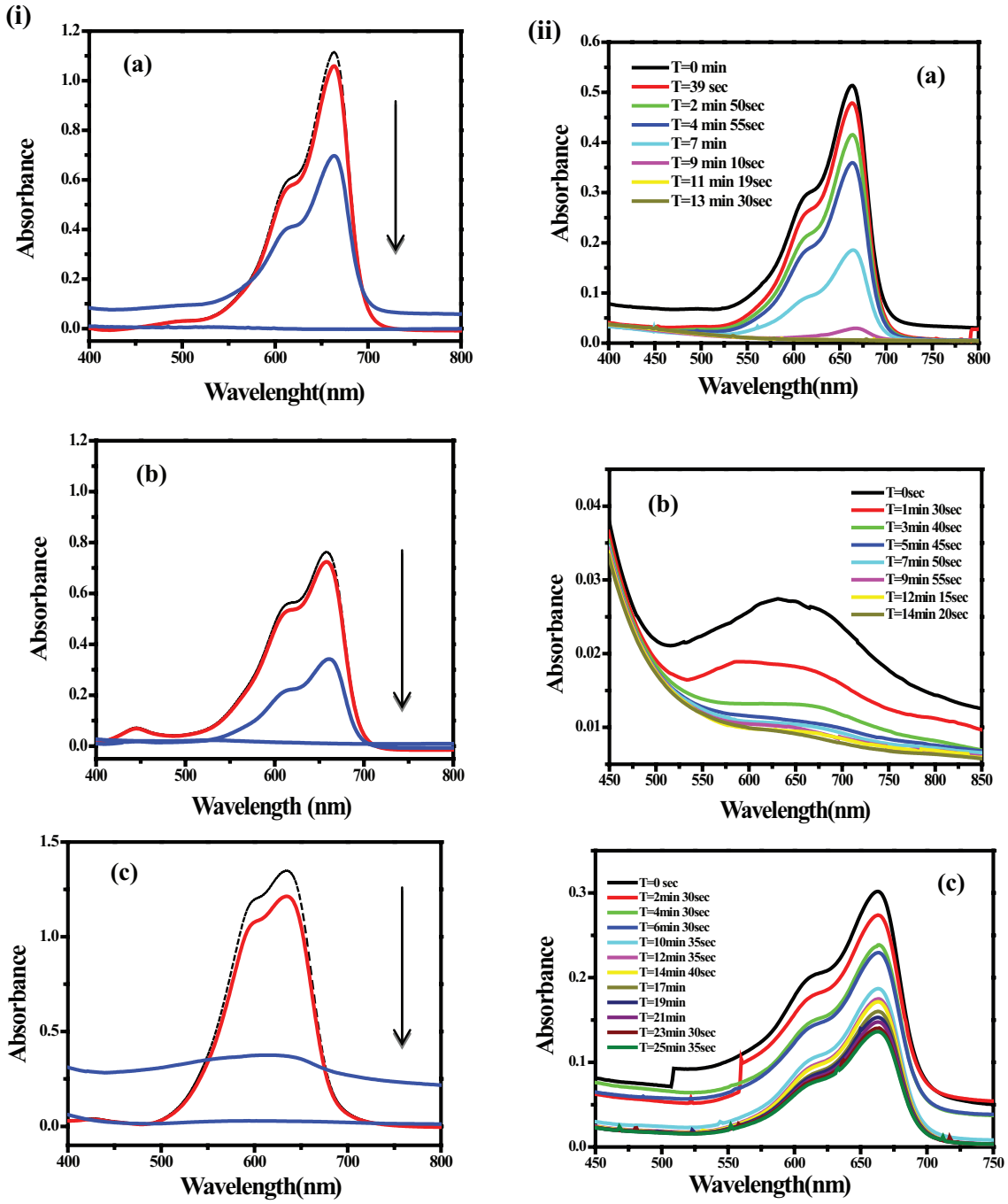

Fig. 6. (i) Reductive degradation of (a) Methylene blue, (b) Methylene green and (c) Nile blue by $NaBH_4$ in the presence of Au NP as catalyst. In all these figures dotted lines indicate the UV-visible spectra of the respective dyes in absence of either $NaBH_4$ or NP catalyst. RED and BLUE lines in these plots indicate the same in presence of $NaBH_4$ and both $NaBH_4$ and Au NP catalyst respectively. (ii) Reductive degradation of (a) Methylene blue, (b) Methylene green and (c) Nile blue by $NaBH_4$ in the presence of Ag NP as catalyst with the variation of time.

Au NP. So the time-dependent kinetics of the reduction process for each of the dyes was carried out with the Ag NP. The progress of the reaction with time has been monitored by UV–Vis spectroscopy and the time of addition of Ag NP has been taken as 0 min. Fig. 6(ii) ((a)–(c)) show the time-dependent UV-visible spectra of $NaBH_4$ reduction of various dyes (MB (a), MG (b), NB (c)) carried out with the Ag NP solution. The plot of the relative absorption intensity vs. wavelength reveals that the complete reduction of MB/NB (Fig. 6(ii) (a) and (c)) which was accomplished in less than

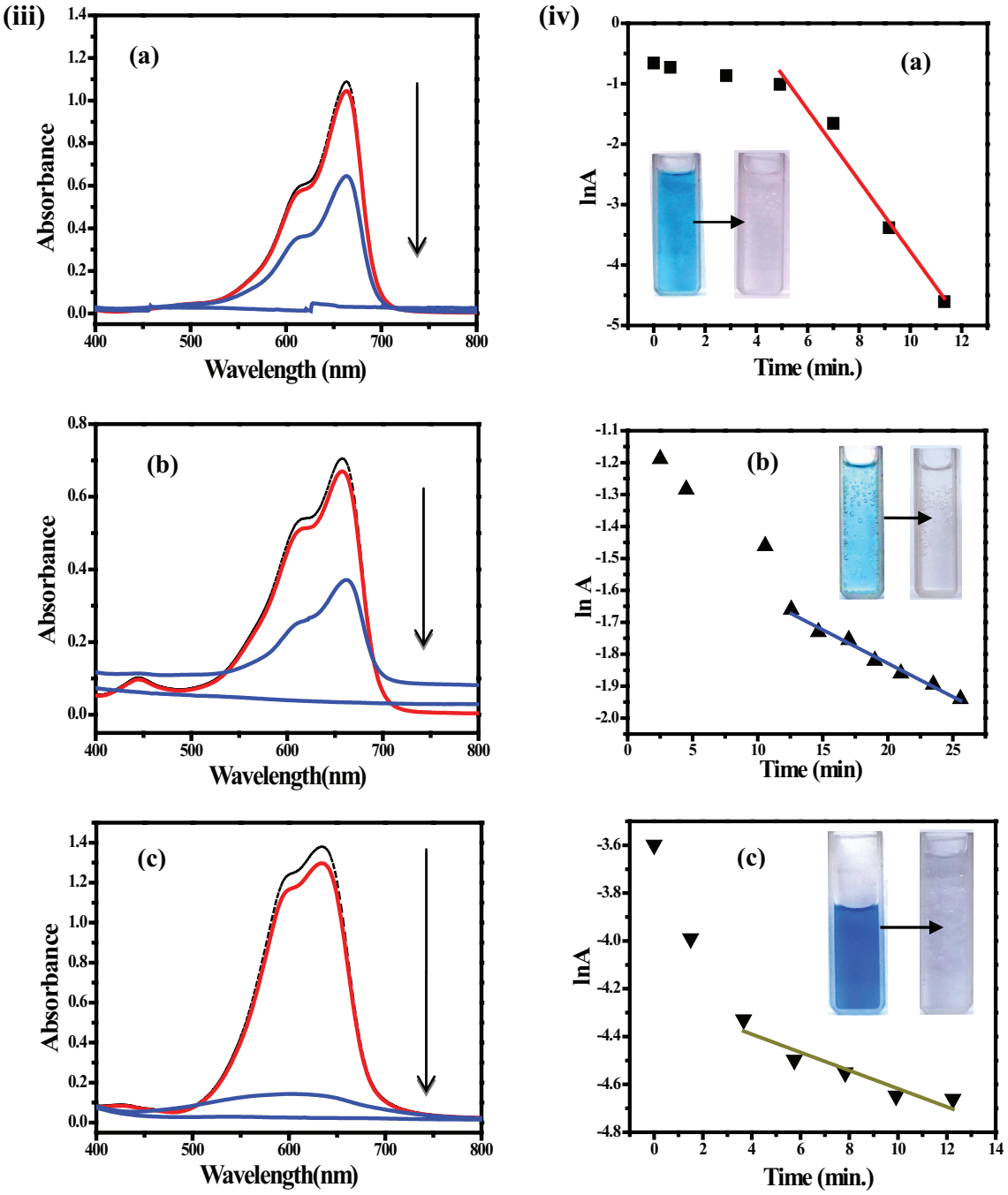

Fig. 6 (*Continued*). (iii) Reductive degradation of (a) Methylene blue, (b) Methylene green and (c) Nile blue by $NaBH_4$ in the presence of bimetallic Au/Ag NP as the catalyst. In all these figures dotted lines indicate the UV-visible spectra of the respective dyes in absence of either $NaBH_4$ or NP catalyst. RED and BLUE lines in these plots indicate the same in presence of $NaBH_4$ and both $NaBH_4$ and NP catalyst respectively. (iv) Reductive degradation kinetics of (a) Methylene blue, (b) Methylene green and (c) Nile blue. Insets of these figures show the change of color of each dye during the degradation process.

Table 3
Kinetic data of the reductive degradation of organic dyes by sodium borohydride in presence of monometallic Ag, Au and bimetallic Au/Ag alloy NPs as catalysts

Organic dyes	First-order rate constant (k_1) (min^{-1})
Methylene blue (MB)	0.586
Methylene green (MG)	0.020
Nile blue (NB)	0.037

15 min while MG took 25 min to complete its reduction in the presence of Ag NP (Fig. 6(ii) (b)).

The UV-visible spectra corresponding to the reductive degradation of MB, MG and NB using Ag/Au alloy NP as catalyst are shown in Fig. 6(iii) ((a)–(c)) and the degradation behavior of the dyes were found to be quite similar, such as Au NP case. Complete catalytic degradation of the dyes occurs within 1 min in the presence of Ag/Au bimetallic alloy NPs. Rate of degradation of the dyes in presence of bimetallic NPs was very fast which is similar to Au NPs.

We have also done kinetic studies with Ag NPs. For Au NPs and bimetallic NPs, the reaction rates are very fast. So we could not perform kinetic studies with these NPs as the catalyst. The kinetic data obtained for MB, MG and NB were fitted to both first order and second order rate equations. Upon further analysis, the data emphasized that the degradation of dyes seemed to follow first order kinetics (Fig. 6(iv) (a) MB, (b) MG, (c) NB). The complete reduction was also visualized when the specific color of the particular dye became colorless (insets of Fig. 6(iv) ((a)–(c))). The results are summarized in Table 3.

4. Conclusion

It is evident that curry leaves acted as the potential green adsorbent for the removal of various dyes from the water. From the adsorption studies on the green adsorbent, it is clear that, the adsorption of dyes was influenced by the pH values, amount of adsorbents and contact time. For optimum removal of dyes, green adsorbent dosage of 8 g L^{-1} was favorable. The uptake of the dye was found to be increased with increasing contact time and the optimum contact time was obtained as 30–60 min. Also, the adsorption of the dyes on this green adsorbent was found to be higher for pH 7. With this easily available and environment friendly green adsorbent, considerable amount of dye removal can be achieved. On the other hand, monometallic Au, Ag and bimetallic Au/Ag alloy NPs synthesized by CAE as green multifunctional agent showed high efficacy toward the borohydride reductive degradation of dyes such as Methylene blue, Methylene green and Nile blue. Both of these two protocols for the removal of toxic organic dyes are very economic and easy to operate using a simple lab set up. Thus, it can substitute other expensive bio-adsorbents and in future, this curry leaves–based green adsorbent can be used for the removal of toxic organic dyes from the industrial waste water.

Acknowledgment

D.K. would like to thank Visva-Bharati for her fellowship. T.M. and A. K. thank UGC for the MANF and UGC-CSIR (NET), respectively, for their fellowships. The authors would like to thank the Department of Chemistry, Visva-Bharati and its DST-FIST and UGC-SAP (Phase-II) programme for necessary infrastructural and instrumental facilities. S.M. would like to thank UGC for financial support (UGC minor project No.: PSW-112/15-16 [ERO] dated 16/11/2016).

References

[1] S.A. Kosa, N.M. Al-sebaii, I.H. Abd El Maksod, E.Z. Hegazy, New method for removal of organic dyes using supported iron oxide as a catalyst, J. Chem., 9 (2016) 1–9.
[2] E. Forgacs, C. Tibor, G. Oros, Removal of synthetic dyes from wastewaters: a review, Environ. Int., 30 (2004) 953–971.
[3] G. Annadurai, M. Chellapandian, M.R.V. Krishnan, Adsorption of Reactive Dye on chitin, Environ. Monit. Assess., 59 (1999) 111–119.
[4] P. Monash, G. Pugazhenthi, Investigation of equilibrium and kinetic parameters of methylene blue adsorption onto MCM-41, Korean J. Chem. Eng., 27 (2010) 1184–1191.
[5] G. Liu, R. Yang, M. Li, Liquid adsorption of basic dye using silica aerogels with different textural properties, J. Non-Cryst. Solids, 356 (2010) 250–257.
[6] S.B. Wang, H.T. Li, Structure directed reversible adsorption of organic dye on mesoporous silica in aqueous solution, Microporous Mesoporous Mater., 97 (2006) 21–26.
[7] M. Anbia, S.A. Hariri, Removal of methylene blue from aqueous solution using nanoporous SBA-3, Desalination, 261 (2010) 61–66.
[8] M.M. Ayad, A.A. El-Nasr, J. Stejskal, Kinetics and isotherm studies of methylene blue adsorption onto polyaniline nanotubes base/silica composite, J. Ind. Eng. Chem., 18 (2012) 1964–1969.
[9] D. Balköse, S. Ulutan, F. Özkan, S. Ülkü, U. Köktürk, Flexible poly (vinyl chloride)-zeolite composites for dye adsorption from aqueous solutions, Sep. Sci. Technol., 31 (1996) 1279–1289.
[10] S. Yetgin, S. Ulutan, D. Balkose, Methylene blue adsorption from aqueous solutions to flexible poly (vinyl chloride) silica composites, J. Vinyl Additive Technol., 21 (2015) 42–50.
[11] O.S. Bello, K.A. Adegoke, A.A. Olaniyan, H. Abdulazeez, Dye adsorption using biomass wastes and natural adsorbents: overview and future prospects, Desal. Wat. Treat., 53 (2013) 1292–1315.
[12] F. Montagnaro, L. Santoro, Reuse of coal combustion ashes as dyes and heavy metal adsorbents: effect of sieving and demineralization on waste properties and adsorption capacity, Chem. Eng. J., 150 (2009) 174–180.
[13] A. Basu, D. Saha, R. Saha, T. Ghosh, B. Saha, A review on sources, toxicity and remediation technologies for removing arsenic from drinking water, Res. Chem. Intermediat., 40 (2014) 447–485.
[14] M.N. Alam, S. Das, S. Batuta, N. Roy, A. Chatterjee, D. Mandal, N.A. Begum, *Murraya koenegii* Spreng. leaf extract: an efficient green multifunctional agent for the controlled synthesis of Au nanoparticles, ACS Sustain. Chem. Eng., 2 (2014) 652–664.
[15] M.B. Ningappa, R. Dinesha, L. Srinivas, Antioxidant and free radical scavenging activities of polyphenol-enriched curry leaf (*Murraya koenigii* L.) extracts, Food Chem., 106 (2008) 720–728.
[16] E.K. Athanassiou, R.N. Grass, W.J. Stark, Large-scale production of carbon-coated copper nanoparticles for sensor applications, Nanotechnology, 17 (2006) 1668–1673.
[17] P.T. Anastas, J.C. Warner, Green Chemistry: Theory and Practice, Oxford University Press, New York, 1998, p. 30.
[18] F. Wu, Q. Yang, Ammonium bicarbonate reduction route to uniform gold nanoparticles and their applications in catalysis and surface-enhanced Raman scattering, Nano Res., 4 (2011) 861–869.
[19] M.N. Alam, S. Batuta, G. Ahamed, S. Das, D. Mandal, N.A. Begum, Tailoring the catalytic activity of Au nanoparticles synthesized by a naturally occurring green multifunctional

agent, Arab. J. Chem., (2016) http://dx.doi.org/10.1016/j.arabjc.2016.02.007.
[20] V.S. Suvith, D. Philip, Catalytic degradation of methylene blue using biosynthesized gold and silver nanoparticles, Spectrochim. Acta Part A, 118 (2014) 526–532.
[21] V.K. Vidhu, D. Philip, Catalytic degradation of organic dyes using biosynthesized silver nanoparticles, Micron, 56 (2014) 54–62.
[22] M. Maham, M. Nasrollahzadeh, S.M. Sajadi, M. Nekoei, Biosynthesis of Ag/reduced graphene oxide/Fe_3O_4 using *Lotus Garcinii* leaf extract and its application as a recyclable nanocatalyst for the reduction of 4-nitrophenol and organic dyes, J. Colloid Interface Sci., 497 (2017) 33.
[23] M. Sajjadi, M. Nasrollahzadeh, S.M. Sajadi, Green synthesis of Ag/Fe_3O_4 nanocomposite using *Euphorbia peplus* Linn leaf extract and evaluation of its catalytic activity, J. Colloid Interface Sci., 497 (2017) 1.
[24] M. Maryami, M. Nasrollahzadeh, E. Mehdipour, S.M. Sajadi, Preparation of the Ag/RGO nanocomposite by use of *Abutilon hirtum* leaf extract: a recoverable catalyst for the reduction of organic dyes in aqueous medium at room temperature, Int. J. Hydrogen Energy, 41 (2016) 21236.
[25] M. Nasrollahzadeh, M. Atarod, B. Jaleh, M. Gandomi, *In situ* green synthesis of Ag nanoparticles on graphene oxide/TiO_2 nanocomposite and their catalytic activity for the reduction of 4-nitrophenol, Congo red and methylene blue, Ceramics Int., 42 (2016) 8587.
[26] A. Hatamifard, M. Nasrollahzadeh, S.M. Sajadi, Biosynthesis, characterization and catalytic activity of an Ag/zeolite nanocomposite for base- and ligand-free oxidative hydroxylation of phenylboronic acid and reduction of a variety of dyes at room temperature, New J. Chem., 40 (2016) 2501.
[27] M. Atarod, M. Nasrollahzadeh, S.M. Sajadi, *Euphorbia heterophylla* leaf extract mediated green synthesis of Ag/TiO_2 nanocomposite and investigation of its excellent catalytic activity for reduction of variety of dyes in water, J. Colloid Interface Sci., 462 (2016) 272.
[28] B. Khodadadi, M. Bordbar, A. Yeganeh-Faal, M.J. Nasrollahzadeh, Green synthesis of Ag nanoparticles/clinoptilolite using *Vaccinium macrocarpon* fruit extract and its excellent catalytic activity for reduction of organic dyes, J. Alloys Compd., 719 (2017) 82.
[29] B. Khodadadi, M. Bordbar, M. Nasrollahzadeh, *Achillea millefolium* L. extract mediated green synthesis of waste peach kernel shell supported silver nanoparticles: application of the nanoparticles for catalytic reduction of a variety of dyes in water, J. Colloid Interface Sci., 493 (2017) 85.
[30] S.S. Momeni. M. Nasrollahzadeh, A. Rustaiyan, Biosynthesis and application of Ag/bone nanocomposite for the hydration of cyanamides in *Myrica gale* L. extract as a green solvent, J. Colloid Interface Sci., 499 (2017) 93.
[31] Z. Issaabadi, M. Nasrollahzadeh, S.M. Sajadi, Efficient catalytic hydration of cyanamides in aqueous medium and in the presence of Naringin sulfuric acid or green synthesized silver nanoparticles by using *Gongronema latifolium* leaf extract, J. Colloid Interface Sci., 503 (2017) 57.
[32] A. Yeganeh-Faal, M. Bordbar, N. Neghadar, M. Nasrollahzadeh, *In situ* green synthesis of Cu nanoparticles supported on natural Natrolite zeolite for the reduction of 4- nitrophenol, congo red and methylene blue, IET Nanobiotechnol., 11 (2017) 669.
[33] A. Rostami-Vartooni, M. Nasrollahzadeh, M. Salavati-Niasari, M. Atarod, Photocatalytic degradation of azo dyes by titanium dioxide supported silver nanoparticles prepared by a green method using *Carpobrotus acinaciformis* extract, J. Alloys Compd., 689 (2016) 15.
[34] A. Rostami-Vartooni, M. Nasrollahzadeh, M. Alizadeh, Green synthesis of perlite supported silver nanoparticles using *Hamamelis virginiana* leaf extract and investigation of its catalytic activity for the reduction of 4-nitrophenol and Congo red, J. Alloys Compd., 680 (2016) 309.
[35] M. Sorbiun, E.S. Mehr, A. Ramazani, S.T. Fardood, Biosynthesis of Ag, ZnO and bimetallic Ag/ZnO alloy nanoparticles by aqueous extract of oak fruit hull (Jaft) and investigation of photocatalytic activity of ZnO and bimetallic Ag/ZnO for degradation of basic violet 3 dye, J. Mater. Sci. – Mater. Electron., 29 (2018) 2806–2814.
[36] S.T. Fardood, A. Ramazani, S.W. Joo, Sol-gel synthesis and characterization of zinc oxide nanoparticles using black tea extract, JACR, 11 (2017) 8–17.
[37] S.T. Fardood, A. Ramazani, S. Moradi, P.A. Asiabi, Green synthesis of zinc oxide nanoparticles using Arabic gum and photocatalytic degradation of direct blue 129 dye under visible light, J. Mater. Sci. - Mater. Electron., 28 (2017) 13596–13601.
[38] S.T. Fardood, A. Ramazani, S. Moradi, A novel green synthesis of nickel oxide nanoparticles using Arabic gum, Chem. J. Moldova, 12 (2017) 115–118.
[39] S.T. Fardood, A. Ramazani, Z. Golfar, S.W. Joo, Green synthesis of Ni-Cu-Zn ferrite nanoparticles using tragacanth gum and their use as an efficient catalyst for the synthesis of polyhydroquinoline derivatives, Appl. Organomet. Chem., 31 (2017) 3823.
[40] S.T. Fardood, A. Ramazani, S.W. Joo, Eco-friendly synthesis of magnesium oxide nanoparticles using Arabic gum, JACR, 12 (2018) 8–15.
[41] M. Sorbiun, E.S. Mehr, A. Ramazani, S.T Fardood, Green synthesis of zinc oxide and copper oxide nanoparticles using aqueous extract of oak fruit hull (Jaft) and comparing their photocatalytic degradation of basic violet 3, Int. J. Environ. Res., 12 (2018) 29–37.
[42] M.A. Hubbe, S.H. Hassan, J. Ducoste, Cellulosic substrates for removal of pollutants from aqueous system, BioResources, 6 (2011) 2161–2287.
[43] I. Langmuir, The constitution and fundamental properties of solids and liquids. Part I. Solids, J. Am. Chem. Soc., 38 (1916) 2221–2295.
[44] A. Torabinejad, N. Nasirizadeh, M.E. Yazdanshenas, H.A. Tayebi, Synthesize and characterization of aminosilane functionalized MCM-41 for removal of anionic dye: kinetic and thermodynamic study, Int. J. Nano Dimension, 7 (2016) 295–307.
[45] H. Freundlich, Kolloidfällung und Adsorption, Angew. Chem. Int. Ed., 1907. https://doi.org/10.1002/ange.19070201805.
[46] S. Mondal, N. Roy, R.A. Laskar, I. Sk, S. Basu, D. Mandal, N.A. Begum, Biogenic synthesis of Ag, Au and bimetallic Au/Ag alloy nanoparticles using aqueous extract of mahogany (*Swietenia mahogani* JACQ.) leaves, Colloids Surf., B, 82 (2011) 497–504.
[47] M.N. Alam, S. Das, S. Batuta, D. Mandal, N.A. Begum, Green-nanochemistry for safe environment: bio-friendly synthesis of fluorescent monometallic (Ag and Au) and bimetallic (Ag/Au alloy) nanoparticles having pesticide sensing activity, J. Nanostruct. Chem., 6 (2016) 373–395.
[48] F.B. Abdur Rahman, M. Akter, M.Z. Abedin, Dyes removal from textile wastewater using orange peels, IJSTR, 2 (2013) 47–50.
[49] H. Bar, D.K. Bhui, G.P. Sahoo, P. Sarkar, S.P. De, A. Misra, Green synthesis of silver nanoparticles using latex of *Jatropha curcas*, Colloids Surf., A, 339 (2009) 134–139.
[50] S.S. Shankar, A. Rai, A. Ahmad, M. Sastry, Rapid synthesis of Au, Ag, and bimetallic Au core–Ag shell nanoparticles using Neem (*Azadirachta indica*) leaf broth, J. Colloid Interface Sci., 275 (2004) 496–502.
[51] P. Mukherjee, A. Ahmad, D. Mandal, S. Senapati, S.R. Sainkar, M.I. Khan, R. Ramani, R. Pasricha, P.V. Ajaykumar, M. Alam, M. Sastry, R. Kumar, Bioreduction of $AuCl^{4-}$ ions by the fungus, *Verticillium* sp. and surface trapping of the gold nanoparticles formed, Angew. Chem. Int. Ed. Engl., 40 (2011) 3585–3588.

Supplementary material

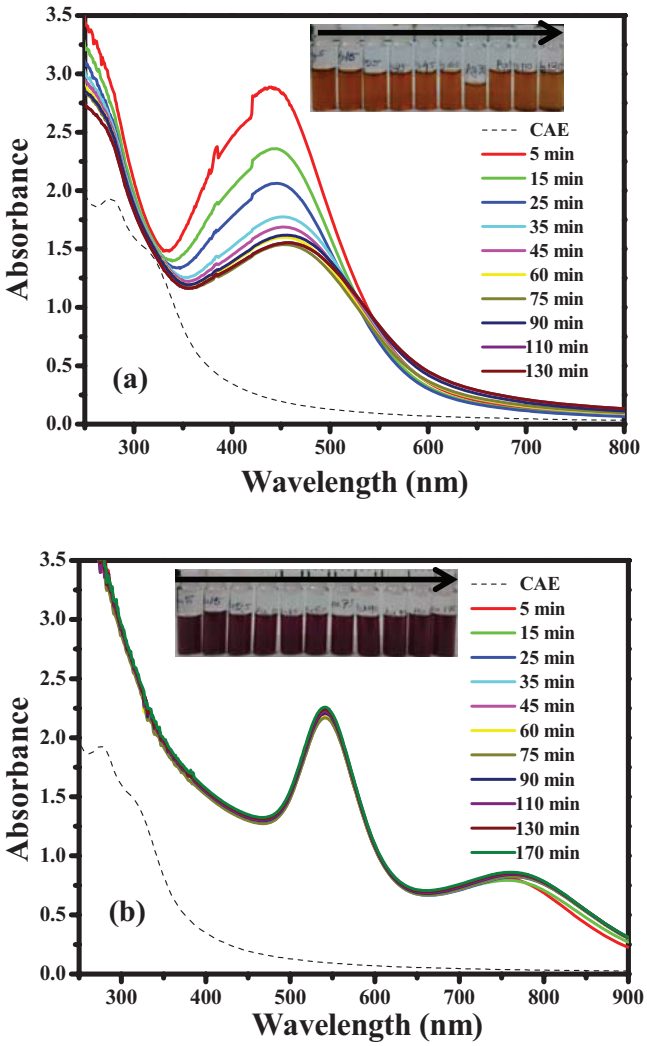

Fig. S1. (a) and (b) UV–Vis spectra of progress of Ag and Au NPs synthesis, respectively, with time prepared by curry leaves aqueous extract (CAE). Broken lines in ((a) and (b)) represent absorbance curve of aqueous solution of CAE. Inset of ((a) and (b)) show the color of the corresponding NP solutions.

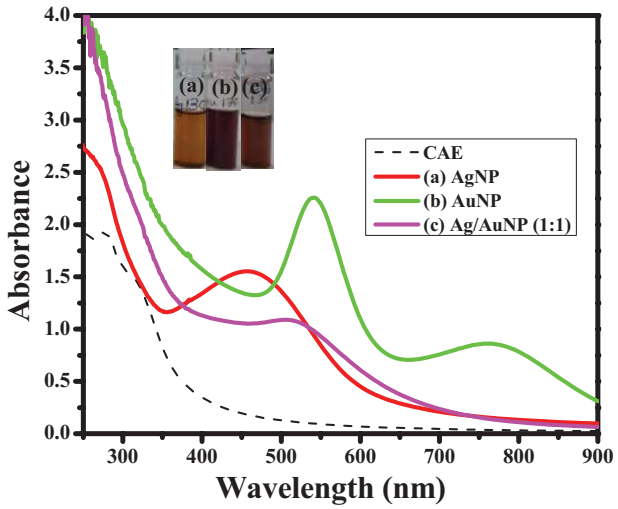

Fig. S2. ((a)–(c)) UV–Vis spectra of monometallic Ag, Au and bimetallic Ag/Au NPs (1:1), respectively, prepared by curry leaves aqueous extract (CAE) with time. Inset of ((a)–(c)) shows the color of the corresponding NPs solutions. Broken lines represent absorbance curve of aqueous solution of CAE.

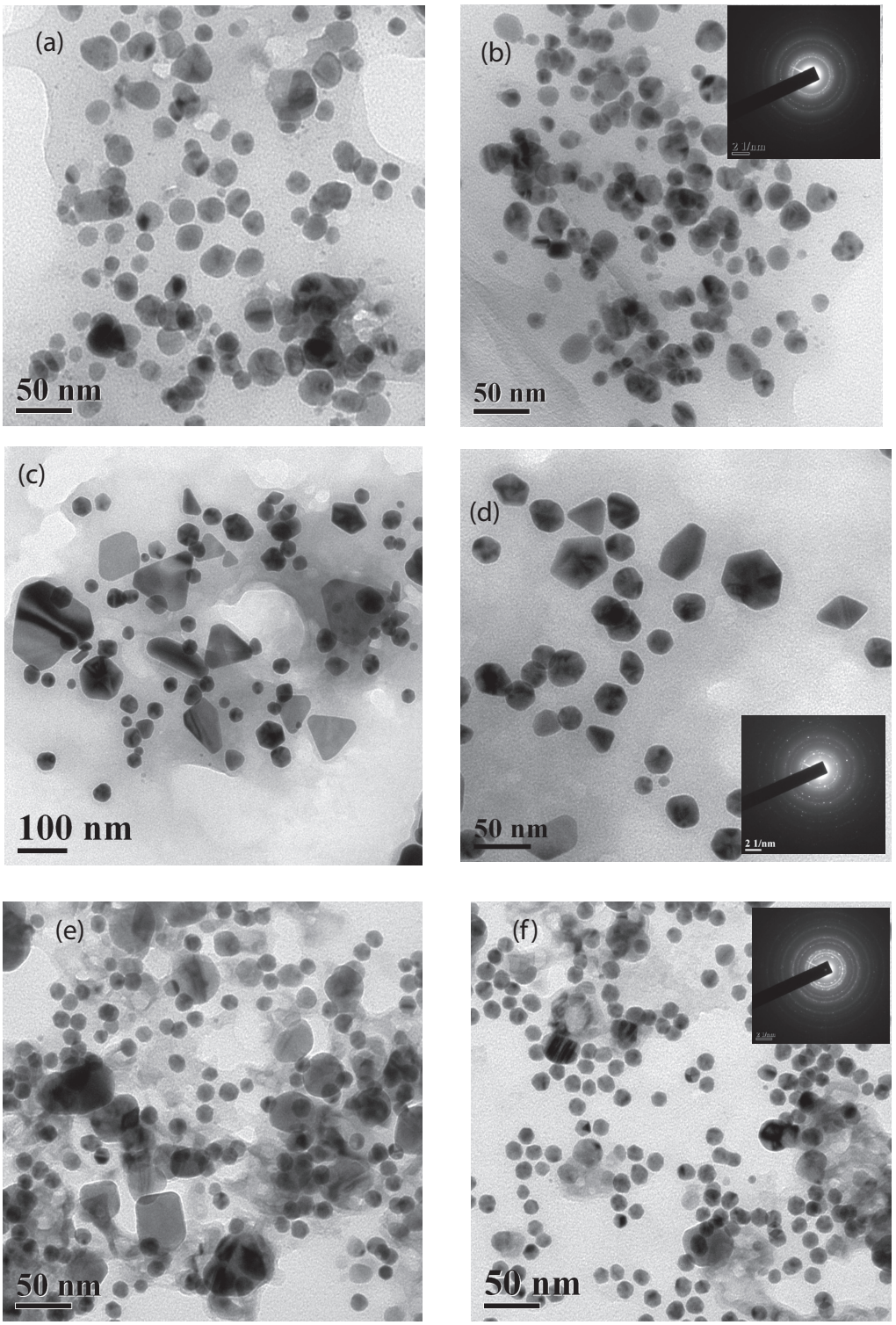

Fig. S3. TEM image of monometallic Ag ((a) and (b)), Au ((c) and (d)) and bimetallic Ag/Au NPs (1:1) ((e) and (f)), respectively, prepared by curry leaves aqueous extract (CAE) with time. Inset of (b), (d) and (f) is selected area electron diffraction images of their corresponding nanoparticles.